5-1-2012

Association of cartilage-specific deletion of peroxisome proliferator-activated receptor γ with abnormal endochondral ossification and impaired cartilage growth and development in a murine model

Roxana Monemdjou
Centre Hospitalier de L'Universite de Montreal

Faezeh Vasheghani
Centre Hospitalier de L'Universite de Montreal

Hassan Fahmi
Centre Hospitalier de L'Universite de Montreal

Gemma Perez
Centre Hospitalier de L'Universite de Montreal

Meryem Blati
Centre Hospitalier de L'Universite de Montreal

Citation of this paper:

Monemdjou, Roxana; Vasheghani, Faezeh; Fahmi, Hassan; Perez, Gemma; Blati, Meryem; Taniguchi, Noboru; Lotz, Martin; St-Arnaud, René; Pelletier, Jean Pierre; Martel-Pelletier, Johanne; Beier, Frank; and Kapoor, Mohit, "Association of cartilage-specific deletion of peroxisome proliferator-activated receptor γ with abnormal endochondral ossification and impaired cartilage growth and development in a murine model" (2012). *Paediatrics Publications*. 775.
https://ir.lib.uwo.ca/paedpub/775

Authors

Roxana Monemdjou, Faezeh Vasheghani, Hassan Fahmi, Gemma Perez, Meryem Blati, Noboru Taniguchi, Martin Lotz, René St-Arnaud, Jean Pierre Pelletier, Johanne Martel-Pelletier, Frank Beier, and Mohit Kapoor

Association of cartilage-specific deletion of peroxisome proliferator-activated receptor γ with abnormal endochondral ossification and impaired cartilage growth and development in a murine model

Roxana Monemdjou[1], Faezeh Vasheghani[1], Hassan Fahmi[1], Gemma Perez[1], Meryem Blati[1], Noboru Taniguchi[2], Martin Lotz[2], René St-Arnaud[4], Jean-Pierre Pelletier[1], Johanne Martel-Pelletier[1], Frank Beier[3], and Mohit Kapoor[1]

[1]Osteoarthritis Research Unit, University of Montreal Hospital Research Centre (CRCHUM) and Department of Medicine, University of Montreal, Montreal, Quebec, Canada, H2L 4M1

[2]Department of Molecular and Experimental Medicine, The Scripps Research Institute, La Jolla, California, USA, 92037

[3]Department of Physiology and Pharmacology, Schulich School of Medicine and Dentistry, University of Western Ontario, London, Ontario, Canada, N6A 5C1

[4]Genetics Unit, Shriners Hospital for Children, Montreal, Quebec, Canada, H3G 1A6

Abstract

Objective—Long bones develop through the strictly regulated process of endochondral ossification within the growth plate, resulting in the replacement of cartilage by bone. Defects in this process result in skeletal abnormalities and can predispose to disease such as osteoarthritis (OA). Studies suggest that activation of the transcription factor peroxisome proliferator activated receptor gamma (PPARγ) is a therapeutic target for OA. In order to devise PPARγ-related therapies in OA and related diseases, it is critical to identify its role in cartilage biology. Therefore, we determined the *in vivo* role of PPARγ in endochondral ossification and cartilage development using cartilage-specific PPARγ knockout (KO) mice.

Methods—Cartilage-specific PPARγ KO mice were generated using LoxP/Cre system. Histomorphometric and immunohistochemical analysis was performed to account for ossification patterns, chondrocyte proliferation, differentiation, hypertrophy, skeletal organization, bone density and calcium deposition. Real-Time PCR and western blotting was performed to determine the expression of key markers involved in endochondral ossification.

Results—PPARγ KO mice exhibited reduced body length, weight, length of long bones, skeletal growth, cellularity, bone density, calcium deposition and trabecular bone thickness, abnormal growth plate organization, loss of columnar organization, shorter hypertrophic zones, and delayed primary and secondary ossification. Immunohistochemistry for Sox9, BrdU, p57, collagen X and PECAM revealed reduction in chondrocyte differentiation and proliferation, and hypertrophy and vascularisation in growth plates of mutant mice. Isolated chondrocytes and cartilage explants from mutant mice showed aberrant expression of ECM markers including aggrecan, collagen II and MMP-13.

Address correspondence and reprint requests to: Mohit Kapoor, PhD, Osteoarthritis Research Unit, University of Montreal Hospital Research Centre (CRCHUM), 1560 Sherbrooke Street East, Pavillion DeSève, 2nd Floor, Montreal, Quebec, Canada, H2L 4M1, Telephone: 1-514-890-8000 ext 25544, Fax: 1-514-412-7583, mohit.kapoor.chum@ssss.gouv.qc.ca.

Conclusion—PPARγ is required for normal endochondral ossification and cartilage development *in vivo*.

INTRODUCTION

Long bones are formed and lengthened through a process termed endochondral ossification whereby a cartilage anlagen grows through chondrocyte proliferation and hypertrophy [1] and, subsequently, cartilage is replaced by bone [2]. In this process, cartilage provides an intermediate template on which bone is laid down [3]. During endochondral bone growth, chondrocytes are organized into three zones within the epiphyses of the cartilage, namely, resting, proliferating, and hypertrophic zones. Resting and proliferating chondrocytes express high levels of aggrecan and collagen type II, the two main components of the cartilage extracellular matrix (ECM), while hypertrophic chondrocytes express collagen type X. Prior to entering the hypertrophic zone, cells exit the cell cycle and begin to differentiate to hypertrophic chondrocytes [4]. Subsequently, they mineralize their surrounding ECM in the cartilage centre and undergo apoptosis [5, 6]. Blood vessels then invade the hypertrophic cartilage region, bringing in osteoblasts and osteoclasts [6]. Osteoclasts degrade mineralized cartilage while osteoblasts replace it with bone tissue [1, 2, 7]. This mineralization process is termed primary ossification [8]. Secondary ossification centres are formed in the epiphyses post-natally [2].

The normal lengthening of long bones depends on the rate of production of hypertrophic chondrocytes from proliferating chondrocytes, the volume increase in hypertrophic chondrocytes, and the number of proliferative cycles a chondrocyte undergoes [4, 9–12]. Disturbances in the fine balance controlling endochondral bone growth result in growth- and development-related abnormalities such as dwarfism and skeletal deformities. Several other signaling molecules, including Indian hedgehog, fibroblast growth factors (FGFs), Akt, and Wnt/β-catenin have been shown to play roles in chondrogenesis and cartilage growth and development [13–16] (Reviewed in [12]). However, the exact mechanisms through which chondrocyte function and behaviour is controlled during chondrogenesis and cartilage growth and development are largely unknown. A better understanding of chondrogenesis and cartilage growth and development will help to advance our knowledge of the pathophysiology of diseases such as OA.

The transcription factor peroxisome proliferator-activated receptor gamma (PPARγ) belongs to the family of ligand-activated nuclear receptors and plays a key role in lipid and glucose homeostasis [17, 18]. It regulates gene expression by binding as a heterodimer to retinoid X receptor. This heterodimer complex acts as a transcriptional regulator upon binding to sequence-specific PPAR response elements in the promoter region of target genes [17, 18]. Recent studies suggest that PPARγ is involved in the maintenance of bone homeostasis by contributing to osteoclastogenic and osteoblastogenic pathways. Mice lacking PPARγ in osteoclasts develop osteopetrosis, which results from impaired osteoclast differentiation [19]. In addition, *in vitro* studies suggest that PPARγ may play a role in chondrocyte biology [20]. However, the specific *in vivo* role of PPARγ in chondrogenesis and cartilage growth and development is still largely unknown. Therefore, this study examined, for the first time, the specific *in vivo* contribution of PPARγ to chondrogenesis and cartilage growth and development using cartilage-specific PPARγ knockout (KO) mice, as global PPARγ KO mice exhibit embryonic lethality due to placental defects [21].

MATERIALS AND METHODS

Materials

C57BL/6-PPARγ^{fl/fl} mice were obtained from Jackson Laboratory (Bar Harbor, Maine). C57BL/6 Col2-Cre transgenic mice were obtained from Shriners Hospital for Children, Montreal, QC, Canada [22]. The following antibodies were used in this study: platelet/endothelial cell adhesion molecule 1 (PECAM-1) #SC-1506, Sox9 #SC-20095, p57 #SC-8298, PPARγ #SC-7273, goat-anti-rabbit #SC-2004, goat-anti-mouse #SC-2005, rabbit-anti-goat #SC-2768 (Santa Cruz Biotechnology, Santa Cruz, California); collagen type X #C-7974, 5-bromo-2'-deoxyuridine (BrdU) #B-8434, Cre #C-7988, MMP-13 #M-4052 (Sigma-Aldrich, Oakville, Ontario); p38 #9212 and phospho-p38 #9216 (Cell Signaling, Danvers, Massachusetts); DMEM and trypsin/EDTA (Wisent, St-Bruno, Quebec).

Generation of cartilage-specific PPARγ KO mice

Genetically modified mice harbouring a cartilage-specific deletion of PPARγ were generated using the Cre Lox methodology in which mice carrying Cre recombinase under the control of the collagen type II promoter were used to induce specific recombination in chondrocytes as previously established [22]. Briefly, mice containing a PPARγ gene flanked by LoxP sites (C57BL/6-PPARγ^{fl/fl}, Jackson Laboratory) were mated with C57BL/6 Col2-Cre transgenic mice [22–24] to generate mice bearing Col2-Cre and a floxed allele in their germline (genotype: PPARγ^{fl/+}, Cre). These mice were backcrossed to homozygote floxed mice in the following cross: PPARγ^{fl/+}, Cre X PPARγ^{fl/fl} to generate mice with both alleles inactivated in chondrocytes (genotype: PPARγ^{fl/fl}, Cre). PPARγ^{fl/fl}, Cre mice are referred to as homozygote PPARγ KO mice, PPARγ^{fl/+} Cre mice are referred to as heterozygote PPARγ KO mice, and PPARγ^{fl/fl} mice without Cre transgene are referred to as control mice.

All procedures involving animals were approved by the *Comité institutionnel de protection des animaux of the* CRCHUM, and the Animal Use Subcommittee of the Canadian Council on Animal Care at the University of Western Ontario. All animal studies including housing and breeding were performed as approved by the aforementioned committees. All mice were kept in a 12 hour light/dark cycle. Food and water were available *ad libitum*.

Primary culture of chondrocytes

Primary chondrocytes were prepared from long bones of embryonic day (E) 16.5 control, heterozygote and homozygote PPARγ KO mice as previously described [25]. Cartilage was dissected from long bones, rinsed in phosphate buffered saline (PBS), and incubated at 37 °C for 15 minutes in trypsin-EDTA followed by digestion with 2 mg/ml collagenase P at 37 °C for 2 hours in Dulbecco's modified Eagle's medium (DMEM) containing 10% fetal bovine serum (FBS), 100 U/ml penicillin, and 100 μg/ml streptomycin under an atmosphere of 5% CO_2. The cell suspension was filtered through a 70-μm cell strainer (Falcon, Fort Worth, Texas), washed, counted and plated. At confluence, the cells were detached and plated for experiments. To retain the phenotype, only first-passage cultured chondrocytes were used throughout the study.

Western blotting

Cells were lysed in Tris-Buffered Saline (TBS) containing 0.1% sodium dodecyl sulfate (SDS), and the protein content of the lysates was determined using bicinchoninic acid protein assay reagent (Thermo Fisher Scientific, Rockford, Illinois) with bovine serum albumin (BSA) as the standard. Cell lysates were adjusted to equal equivalents of protein and then were applied to SDS-polyacrylamide gels (10%) for electrophoresis. Next, the

proteins were electroblotted onto polyvinylidene fluoride membranes. After the membranes were blocked in 10mM TBS containing 0.1% Tween-20 (TBS-T) and 5% skim milk, the membranes were probed for 1.5 hours with the respective primary antibody (anti-PPARγ; 1:1000 dilution) in TBS-T. After washing the membranes with TBS-T, the membranes were incubated overnight with the appropriate secondary antibody in TBS-T containing 5% skim milk at 4 °C. After further washing with TBS-T, protein bands were visualized with an enhanced chemiluminescence system using a Bio-Rad (Mississauga, Ontario) Chemidoc Apparatus.

RNA isolation and real-time polymerase chain reaction

Total RNA was isolated from chondrocytes or cartilage explants using TRIzol (Invitrogen, Burlington, Ontario) and RNeasy (QIAGEN, Toronto, Ontario) according to the manufacturers' recommendations, reverse transcribed and amplified using the TaqMan Assays-on-Demand (Applied Biosystems, Streetsville, Ontario) in a reaction solution containing two unlabeled primers and a 6-carboxyfluorescein-labeled TaqMan MGB probe [26, 27]. Samples were combined with One-Step MasterMix (Eurogentec, San Diego, California). Amplified sequences were detected using the ABI Prism 7900HT sequence detector (Applied Biosystems) according to the manufacturer's instructions. The expression values were standardized to values obtained with control glyceraldehyde 3-phosphate dehydrogenase (GAPDH) RNA primers using the ΔCt method. All primers and probe sets were obtained from Applied Biosystems and data were normalized to GAPDH mRNA levels and represent averages and standard error of the mean (SEM) from direct comparison of KO and control littermates. Statistical significance of real time polymerase chain reaction (qPCR) results was determined by two-way analysis of variance with the Bonferroni post-test using GraphPad Prism 3.00 for Windows.

Skeletal staining

Newborn mice were skinned, eviscerated, and dehydrated in 95% ethanol and acetone overnight. Skeletons were stained with 0.015% alcian blue, 0.05% alizarin red, and 5% acetic acid in 70% ethanol for several days. Skeletons were then cleared in 1% KOH, passed through a decreasing KOH series and stored in glycerol/ethanol (1:1) [23, 28].

Histological and immunohistochemistry studies

Freshly dissected mouse long bones were fixed with 10% neutral buffered formalin and decalcified with 0.1 M EDTA at room temperature before paraffin embedding and sectioning at the Centre for Bone and Periodontal Research at McGill University (Montreal, QC, Canada). Sections (5 μm) were deparaffinized in xylene followed by a graded series of alcohol washes. Sections were stained with Safranin-O/Fast Green (Sigma-Aldrich, Oakville, Ontario) according to the manufacturer's recommendations. For immunohistochemistry (IHC) analysis, the Dakocytomation (Dako, Burlington, Ontario) labeled streptavidin biotin + System-horseradish peroxidase kit was used following the manufacturer's recommended protocol. Briefly, endogenous peroxide was blocked for 5 minutes using 3% H_2O_2. Nonspecific immunoglobulin G binding was blocked by incubating sections with BSA (0.1%) in PBS for 1 hour. Sections were then incubated with the primary antibody in a humidified chamber and left overnight at 4 °C. Next, sections were incubated with biotinylated link for 30 minutes followed by streptavidin for 1 hour. The diaminobenzidine tetrahydrochloride chromogen substrate solution was then added until sufficient color developed.

BrdU labeling

For BrdU labeling, pregnant female mice were injected one day before being sacrificed i.p. with BrdU at a dose of 0.01 ml/g. BrdU was detected in paraffin sections using an anti-BrdU antibody through IHC as detailed above.

Bone mineralization

Freshly dissected mouse long bones were fixed with 10% neutral buffered formalin before plastic embedding, sectioning, and staining at the Centre for Bone and Periodontal Research at McGill University (Montreal, QC, Canada). Sections (5 μm) were stained with von Kossa to determine calcium deposition in the bone, Goldner to determine bone density, and Safranin-O/Fast Green to determine trabecular bone thickness. Bone density and trabecular bone thickness were quantified using Bioquant Osteo II software as previously described [29].

Cartilage explant studies

Cartilage explant studies were conducted using femoral head cartilage from 3-week-old control and homozygote PPARγ KO mice. Cartilage was extracted, rinsed in PBS and RNA was isolated and subjected to qPCR using specific primers as described above.

Statistical analysis

Statistical analysis was evaluated by the two-tailed Student's t-test. $P < 0.05$ was considered statistically significant.

RESULTS

Characterization of cartilage-specific PPARγ KO mice

Due to the fact that global PPARγ KO mice die as a result of embryonic lethality, the LoxP/ Cre system was used to generate cartilage-specific PPARγ conditional KO mice. Mice containing a PPARγ gene flanked by LoxP sites (PPARγ$^{fl/fl}$) were mated with mice carrying Cre recombinase under the control of the collagen type II promoter to induce specific recombination in chondrocytes [22]. Generation of conditional KO mice was first determined by tail DNA genotyping, which confirmed the presence of the Cre transgene in heterozygote (PPARγ$^{fl/w}$ Cre) and homozygote (PPARγ$^{f/f}$ Cre) PPARγ KO mice and its absence in WT (wild-type) (control) mice (Figure 1A). Loss of PPARγ expression in chondrocytes isolated from homozygote and heterozygote PPARγ KO versus control mice was confirmed by Western blotting (Figure 1B) and qPCR (Figure 1C). Additionally, IHC studies performed on femurs of post-natal day (P) 0 control mice demonstrated strong expression of PPARγ in resting and hypertrophic chondrocytes of the growth plate. However, PPARγ positive chondrocytes were undetectable in the resting and hypertrophic zones of the growth plate of homozygote PPARγ KO mice, thus confirming that recombination occurred with high efficiency (Figure 1D).

Cartilage-specific deletion of PPARγ results in reduced growth

We first determined the effect of cartilage-specific ablation of PPARγ on body length, body weight, and skeletal growth of mice. Analyses of newborn litters demonstrated growth retardation in homozygote PPARγ KO mice compared to control mice (Figure 2A). Whole-mount skeletal staining with alcian blue and alizarin red confirmed that newborn homozygote PPARγ KO mice show reduced skeletal growth compared to control mice and skeletal staining in some regions of the limbs in mutant mice was weaker compared to control mice (Figure 2B). Measurements of growth over 42 days post-birth demonstrated that homozygote PPARγ KO mice had significantly reduced body length (Figure 2C) and

weight (Figure 2D) compared to control mice. Measurements of individual bones demonstrated that homozygote PPARγ KO mice had significantly reduced length of tibiae and femurs at time of birth (Figure 2E). No significant differences in the viability of mice were observed. A consistent pattern of growth and weight retardation was observed in both genders.

PPARγ-deficient mice show delayed ossification and disorganization of growth plates

We further examined the effect of PPARγ deficiency on the organization of growth plates and ossification patterns. Histological analysis by Safranin-O/Fast Green staining demonstrated that femurs of E16.5 homozygote PPARγ KO mice exhibit reduced length and delayed primary ossification compared to control mice (Figure 3A). In addition, femurs of P14 homozygote PPARγ KO mice exhibited delayed secondary ossification compared to control mice (Figure 3B).

Blinded histological analyses were also performed to examine growth plate organization on a cellular level at time of birth. Safranin-O/Fast Green staining of P0 mouse femurs of homozygote PPARγ KO mice demonstrated growth plate defects, which is associated with hypocellularity in all three zones, loss of columnar organization in the proliferating zone, altered chondrocyte shape in the hypertrophic zone, and a shortened hypertrophic zone compared to control mice (Figure 3C,D).

Cartilage-specific deletion of PPARγ results in reduced chondrocyte proliferation, differentiation, hypertrophy and vascular invasion

Subsequently, we determined if PPARγ deficiency altered chondrocyte differentiation, proliferation, hypertrophy and vascular invasion. IHC using antibodies against Sox9 (Figure 4A), a marker of early chondrocyte differentiation, BrdU (Figure 4B), a marker of proliferation, and p57 (Figure 4C), a cell cycle inhibitor required for normal hypertrophic differentiation, revealed that femurs of E16.5 homozygote PPARγ KO mice exhibit reduced chondrocyte differentiation and proliferation as demonstrated by a reduced percentage of positive cells compared to control mice. IHC using collagen type X, a marker of chondrocyte hypertrophy, demonstrated that the femurs of E16.5 homozygote PPARγ KO mice exhibit reduced chondrocyte hypertrophy compared to control mice (Figure 4D). IHC for PECAM, a cell surface marker for endothelial cells and a marker of new blood vessel formation, further demonstrated reduced vascular invasion in the femurs of E16.5 homozygote PPARγ KO mice compared to control mice (Figure 4E).

Cartilage-specific deletion of PPARγ causes reduced bone density

We further investigated whether the loss of PPARγ resulted in abnormal calcium deposition and bone density. Two bone mineralization staining methods, von Kossa (Figure 5A) and Goldner (Figure 5B), in combination with measurements to quantify bone density (Figure 5C) using Bioquant Osteo II software, demonstrated that P0 homozygote PPARγ KO mouse femurs exhibit reduced calcium deposition and bone density, respectively, compared to control mice. Measurements using Bioquant Osteo II software to quantify trabecular bone thickness in P40 and P70 mice further demonstrated that homozygote PPARγ KO mice display significantly reduced trabecular bone thickness compared to control mice (Figure 5D).

PPARγ-deficiency results in reduced expression of aggrecan and collagen type II, and increased expression of MMP-13

We next isolated chondrocytes from E16.5 control and homozygote PPARγ KO mice (Figure 6A), and femur head cartilage explants from 3-week-old control and homozygote

PPARγ KO mice (Figure 6B) and examined the expression of the ECM proteins, aggrecan and collagen type II, and the catabolic factor MMP-13. Our analyses indicated that homozygote PPARγ KO mouse chondrocytes and cartilage explants exhibit significantly reduced expression of aggrecan and collagen type II, and significantly increased expression of MMP-13 compared to control mouse chondrocytes and cartilage explants.

DISCUSSION

Our results, for the first time, demonstrate an important *in vivo* role of PPARγ in endochondral ossification and cartilage growth and development through the use of cartilage-specific PPARγ KO mice. We show that genetic ablation of PPARγ in cartilage *in vivo* results in marked alterations in the process of endochondral ossification, and cartilage and long bone development, with specific alterations at the tissue, cellular, and molecular levels. PPARγ deficiency caused reduced growth and skeletal size, shorter length of long bones, delayed primary and secondary ossification, disorganization of growth plates accompanied by hypocellularity, reduced chondrocyte proliferation, differentiation and hypertrophy, delayed vascular invasion, decreased bone density, calcium deposition and trabecular bone thickness, and aberrant expression of key markers involved in skeletogenesis (Sox9, p57, and collagen type X) as well as ECM synthesis (aggrecan and collagen type II) and degradation (MMP-13) products. Collectively, our results demonstrate that PPARγ plays a pivotal role in coordinating diverse aspects of skeletal morphogenesis.

As demonstrated by skeletal staining and measurements, cartilage-specific deletion of PPARγ resulted in abnormal endochondral bone growth, including reduced body size in terms of height and weight as well as reduced skeletal size and length of long bones. Histological analyses further revealed that PPARγ deficiency caused delayed primary and secondary ossification and disorganization of the growth plates. All three zones of the cartilage epiphyses of mutant mice showed signs of highly disorganized growth plates, including hypocellularity and reduced chondrocyte proliferation, differentiation and hypertrophy. Since the normal lengthening of long bones depends on the rate of production of hypertrophic chondrocytes from proliferating chondrocytes, the increased volume of hypertrophic chondrocytes, and the number of proliferative cycles a chondrocyte undergoes [9–12], improper coordination of these variables results in abnormal bone length by hindering mineralization, apoptosis, vascular invasion, and thus, overall endochondral bone development.

Some of the key essential factors required for normal ossification, ECM production, and vascularization processes during early development of cartilage and bone include Sox9, p57, aggrecan, collagen type II, and collagen type X. During chondrogenesis, chondrocytes begin expressing Sox9, a chondrogenic transcription factor that is essential for proliferation and differentiation of chondrocytes. Within the growth plate, Sox9 is expressed in resting and proliferating chondrocytes and regulates the expression of genes encoding aggrecan and collagen type II, the two main components of the cartilage ECM [30–32]. p57 is a cell cycle inhibitor essential for cell cycle exit and onset of hypertrophic differentiation. Collagen type X is a cartilage ECM component unique to the hypertrophic zone and serves as a marker of terminally differentiated hypertrophic chondrocytes [33]. In the final step of endochondral bone development, chondrocytes undergo hypertrophy and produce a calcified, cartilaginous ECM, and angiogenic factors, which initiate and propagate vascular invasion. As a result, avascular cartilage is replaced by densely vascularized bone.

Delayed ossification and growth plate abnormalities in PPARγ mutant mice can be explained by the abnormal expression of Sox9, p57, and collagen type X. Our results show that the growth plates of homozygote PPARγ KO mice exhibit significantly reduced

expression of Sox9 and p57, thus affecting the normal sequence of chondrocyte proliferation, differentiation, and hypertrophy. In addition, the growth plates of homozygote PPARγ KO mice exhibit significantly reduced expression of PECAM, indicating delayed vascularization. Growth plates of homozygote PPARγ KO mice showed reduced expression of collagen type X. Collagen type X facilitates endochondral ossification by regulating matrix mineralization and compartmentalizing matrix components [34]. Mice with altered collagen type X function exhibit skeletal defects including compressed growth plates with reduced proliferative and hypertrophic zones, and trabecular bone thickness [35–37]. Therefore, reduced length of long bones, bone density and trabecular bone thickness may in part be dependent on decreased collagen type X expression upon genetic deletion of PPARγ.

We have previously observed a close relationship between PPARγ and p38 signalling. We have shown that PPARγ expression is suppressed by p38 activity. We examined show that PPARγ deficient chondrocytes (E16.5) show increased phosphorylation of p-38 and reduction in the mRNA expression of Indian Hedgehog (Ihh). Previous study using transgenic mice that specifically expresses a constitutively active mutant of MKK6 in chondrocytes that specifically activates p38 results in mice exhibiting a dwarf phenotype associated with reduction in chondrocyte proliferation, inhibition of hypertrophic chondrocyte differentiation, and a delay in primary and secondary ossification (Zhang et al., 2006 PNAS), a similar phenotype we observe with PPARγ-deficient mice. Ihh is a key regulator of normal endochondral bone and skeletal development (St-Jacques et al., 1999, Genes & Dev). We and others have shown that p38 negatively regulates the expression of Ihh both in vitro (Stanton and Beier, 2007, Exp. Cell Res) and in vivo (Zhang et al., 2006 PNAS). Here we show that PPARγ deficient chondrocytes exhibit decreased expression of Ihh, suggesting that inactivation of PPARγ and subsequent increase in the phosphorylation of p38 may account for repression of Ihh and ultimately contributing towards abnormal endochondral ossification observed in PPARγ-deficient mice.

It should be mentioned that previous studies have shown that PPARγ activation suppresses collagen type X expression and other markers of hypertrophic chondrocyte differentiation [20, 38]. At first glance, this appears to be contradictory to the delay in hypertrophic differentiation upon inactivation of PPARγ that we observed here. However, several possibilities could explain these apparent discrepancies. First, it is possible that there is an optimal level of PPARγ activity to promote hypertrophy and that both overactivation and inactivation suppress this process. Second, it is possible that reduced hypertrophy in these two settings is due to different mechanisms; PPARγ activation might directly suppress hypertrophy, while the smaller hypertrophic zone in cartilage-specific PPARγ KO mice could be secondary to reduced chondrocyte proliferation (e.g. less cells entering the hypertrophic zone). Further studies will be required to decipher the mechanisms involved.

In closing, our results, for the first time, demonstrate that PPARγ is a critical regulator of endochondral cartilage health and physiology in early growth and development. Collectively, our results demonstrate that PPARγ plays a pivotal role in coordinating diverse aspects of skeletal morphogenesis. A better understanding of the role of PPARγ in cartilage biology will enable us to devise appropriate PPARγ related therapeutic strategies against diseases such as OA and related disorders.

Acknowledgments

References

1. Woods A, Wang G, Beier F. Regulation of chondrocyte differentiation by the actin cytoskeleton and adhesive interactions. J Cell Physiol. 2007; 213(1):1–8. [PubMed: 17492773]

2. Olsen BR, Reginato AM, Wang W. Bone development. Annu Rev Cell Dev Biol. 2000; 16:191–220. [PubMed: 11031235]

3. Erlebacher A, Filvaroff EH, Gitelman SE, Derynck R. Toward a molecular understanding of skeletal development. Cell. 1995; 80(3):371–378. [PubMed: 7859279]

4. Beier F. Cell-cycle control and the cartilage growth plate. J Cell Physiol. 2005; 202(1):1–8. [PubMed: 15389526]

5. Shapiro IM, Adams CS, Freeman T, Srinivas V. Fate of the hypertrophic chondrocyte: microenvironmental perspectives on apoptosis and survival in the epiphyseal growth plate. Birth Defects Res C Embryo Today. 2005; 75(4):330–339. [PubMed: 16425255]

6. Karsenty G, Wagner EF. Reaching a genetic and molecular understanding of skeletal development. Dev Cell. 2002; 2(4):389–406. [PubMed: 11970890]

7. Gerber HP, Vu TH, Ryan AM, Kowalski J, Werb Z, Ferrara N. VEGF couples hypertrophic cartilage remodeling, ossification and angiogenesis during endochondral bone formation. Nat Med. 1999; 5(6):623–628. [PubMed: 10371499]

8. van der Eerden BC, Karperien M, Wit JM. Systemic and local regulation of the growth plate. Endocr Rev. 2003; 24(6):782–801. [PubMed: 14671005]

9. Hunziker EB. Mechanism of longitudinal bone growth and its regulation by growth plate chondrocytes. Microsc Res Tech. 1994; 28(6):505–519. [PubMed: 7949396]

10. Wilsman NJ, Farnum CE, Green EM, Lieferman EM, Clayton MK. Cell cycle analysis of proliferative zone chondrocytes in growth plates elongating at different rates. J Orthop Res. 1996; 14(4):562–572. [PubMed: 8764865]

11. Wilsman NJ, Farnum CE, Leiferman EM, Fry M, Barreto C. Differential growth by growth plates as a function of multiple parameters of chondrocytic kinetics. J Orthop Res. 1996; 14(6):927–936. [PubMed: 8982136]

12. Kronenberg HM. Developmental regulation of the growth plate. Nature. 2003; 423(6937):332–336. [PubMed: 12748651]

13. Naski MC, Colvin JS, Coffin JD, Ornitz DM. Repression of hedgehog signaling and BMP4 expression in growth plate cartilage by fibroblast growth factor receptor 3. Development. 1998; 125(24):4977–4988. [PubMed: 9811582]

14. St-Jacques B, Hammerschmidt M, McMahon AP. Indian hedgehog signaling regulates proliferation and differentiation of chondrocytes and is essential for bone formation. Genes Dev. 1999; 13(16):2072–2086. [PubMed: 10465785]

15. Andrade AC, Nilsson O, Barnes KM, Baron J. Wnt gene expression in the post-natal growth plate: regulation with chondrocyte differentiation. Bone. 2007; 40(5):1361–1369. [PubMed: 17337262]

16. Ulici V, Hoenselaar KD, Agoston H, McErlain DD, Umoh J, Chakrabarti S, Holdsworth DW, Beier F. The role of Akt1 in terminal stages of endochondral bone formation: angiogenesis and ossification. Bone. 2009; 45(6):1133–1145. [PubMed: 19679212]

17. Dubuquoy L, Dharancy S, Nutten S, Pettersson S, Auwerx J, Desreumaux P. Role of peroxisome proliferator-activated receptor gamma and retinoid X receptor heterodimer in hepatogastroenterological diseases. Lancet. 2002; 360(9343):1410–1418. [PubMed: 12424006]

18. Belvisi MG, Hele DJ, Birrell MA. Peroxisome proliferator-activated receptor gamma agonists as therapy for chronic airway inflammation. Eur J Pharmacol. 2006; 533(1–3):101–109. [PubMed: 16458290]

19. Wan Y, Chong LW, Evans RM. PPAR-gamma regulates osteoclastogenesis in mice. Nat Med. 2007; 13(12):1496–1503. [PubMed: 18059282]

20. Stanton LA, Li JR, Beier F. PPARgamma2 expression in growth plate chondrocytes is regulated by p38 and GSK-3. J Cell Mol Med. 2010; 14(1–2):242–256. [PubMed: 20414969]

21. Barak Y, Nelson MC, Ong ES, Jones YZ, Ruiz-Lozano P, Chien KR, Koder A, Evans RM. PPAR gamma is required for placental, cardiac, and adipose tissue development. Mol Cell. 1999; 4(4): 585–595. [PubMed: 10549290]

22. Terpstra L, Prud'homme J, Arabian A, Takeda S, Karsenty G, Dedhar S, St-Arnaud R. Reduced chondrocyte proliferation and chondrodysplasia in mice lacking the integrin-linked kinase in chondrocytes. J Cell Biol. 2003; 162(1):139–148. [PubMed: 12835312]

23. Wang G, Woods A, Agoston H, Ulici V, Glogauer M, Beier F. Genetic ablation of Rac1 in cartilage results in chondrodysplasia. Dev Biol. 2007; 306(2):612–623. [PubMed: 17467682]

24. Solomon LA, Li JR, Berube NG, Beier F. Loss of ATRX in chondrocytes has minimal effects on skeletal development. PLoS One. 2009; 4(9):e7106. [PubMed: 19774083]

25. Woods A, Beier F. RhoA/ROCK signaling regulates chondrogenesis in a context-dependent manner. J Biol Chem. 2006; 281(19):13134–13140. [PubMed: 16565087]

26. Woods A, Wang G, Beier F. RhoA/ROCK signaling regulates Sox9 expression and actin organization during chondrogenesis. J Biol Chem. 2005; 280(12):11626–11634. [PubMed: 15665004]

27. James CG, Appleton CT, Ulici V, Underhill TM, Beier F. Microarray analyses of gene expression during chondrocyte differentiation identifies novel regulators of hypertrophy. Mol Biol Cell. 2005; 16(11):5316–5333. [PubMed: 16135533]

28. Yan Q, Feng Q, Beier F. Endothelial nitric oxide synthase deficiency in mice results in reduced chondrocyte proliferation and endochondral bone growth. Arthritis Rheum. 2010; 62(7):2013–2022. [PubMed: 20506524]

29. Amiable N, Martel-Pelletier J, Lussier B, Kwan Tat S, Pelletier JP, Boileau C. Proteinase-activated receptor-2 gene disruption limits the effect of osteoarthritis on cartilage in mice: a novel target in joint degradation. J Rheumatol. 2011; 38(5):911–920. [PubMed: 21285164]

30. Horton, WA. Cartilage Morphology. In: Royce, PM.; Steinman, B., editors. Extracellular Matrix and Heritable Disorder of Connective Tissue. New York: Alan R. LIss; 1993. p. 73-84.

31. Doege, KJ. Aggrecan. In: Kreis, T.; Vale, R., editors. Guidebook to the Extracellular Matrix, Anchor and Adhesion. 2 edn. A Sambrook and Tooze Publication at Oxford University Press; 1999.

32. Ruoslahti E, Yamaguchi Y. Proteoglycans as modulators of growth factor activities. Cell. 1991; 64(5):867–869. [PubMed: 2001586]

33. Schmid TM, Linsenmayer TF. Immunohistochemical localization of short chain cartilage collagen (type X) in avian tissues. J Cell Biol. 1985; 100(2):598–605. [PubMed: 2578471]

34. Kwan KM, Pang MK, Zhou S, Cowan SK, Kong RY, Pfordte T, Olsen BR, Sillence DO, Tam PP, Cheah KS. Abnormal compartmentalization of cartilage matrix components in mice lacking collagen X: implications for function. J Cell Biol. 1997; 136(2):459–471. [PubMed: 9015315]

35. Gress CJ, Jacenko O. Growth plate compressions and altered hematopoiesis in collagen X null mice. J Cell Biol. 2000; 149(4):983–993. [PubMed: 10811836]

36. Jacenko O, Roberts DW, Campbell MR, McManus PM, Gress CJ, Tao Z. Linking hematopoiesis to endochondral skeletogenesis through analysis of mice transgenic for collagen X. Am J Pathol. 2002; 160(6):2019–2034. [PubMed: 12057907]

37. Jacenko O, LuValle PA, Olsen BR. Spondylometaphyseal dysplasia in mice carrying a dominant negative mutation in a matrix protein specific for cartilage-to-bone transition. Nature. 1993; 365(6441):56–61. [PubMed: 8361538]

38. Wang L, Shao YY, Ballock RT. Peroxisome proliferator activated receptor-gamma (PPARgamma) represses thyroid hormone signaling in growth plate chondrocytes. Bone. 2005; 37(3):305–312. [PubMed: 16023420]
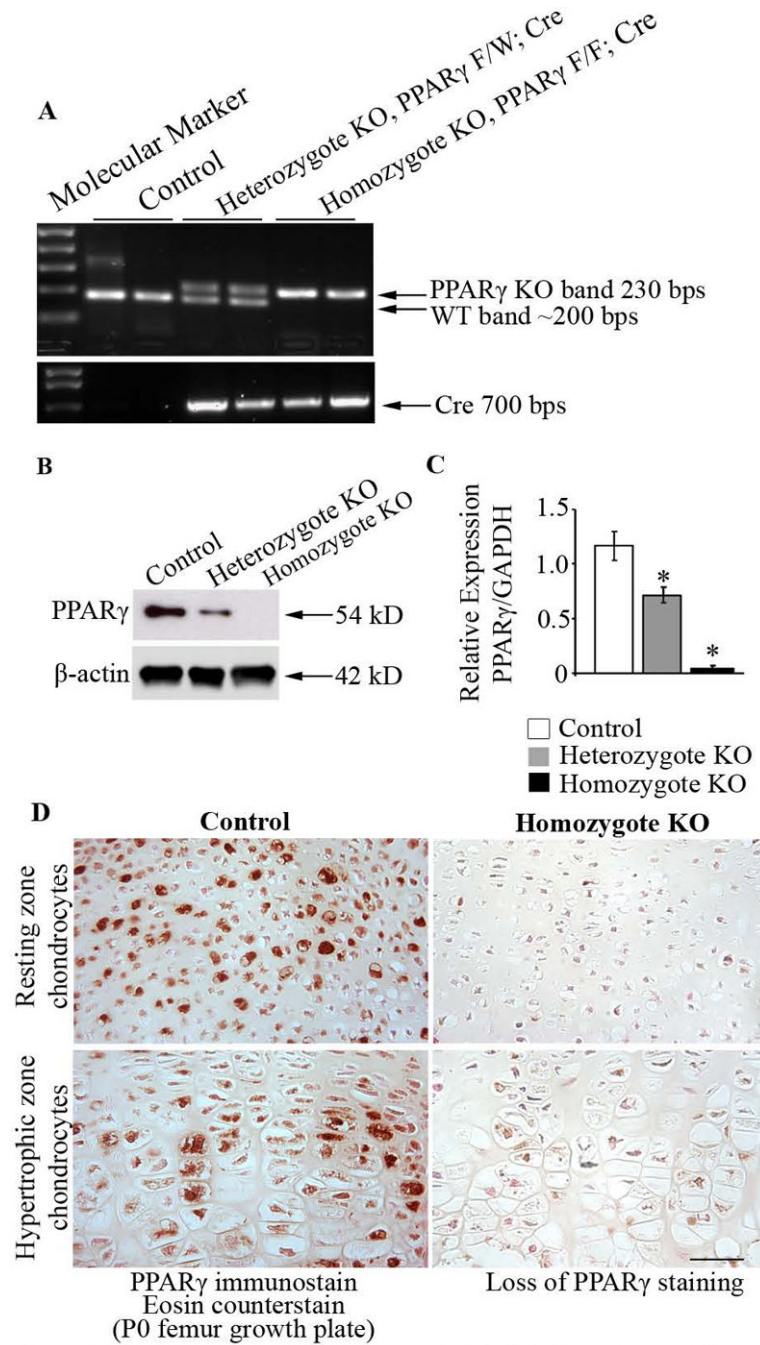
Figure 1.
Characterization of cartilage-specific PPARγ KO mice. (A) Genotyping confirmed presence of Cre transgene in P0 heterozygote and homozygote KO mice and its absence in control mice. PPARγ KO band was detected at 230 bps, WT band was detected at ~200 bps, and Cre band was detected at 700 bps. (B) Western blotting performed on isolated chondrocytes demonstrated reduced expression and complete absence of PPARγ in heterozygote and homozygote PPARγ KO mice, respectively, compared to control mice. (C) RT-PCR on isolated chondrocytes confirmed reduction of PPARγ mRNA levels by >96% in homozygote PPARγ KO mice compared to control mice. Representative data from n=6 independent isolated chondrocytes per group. Bar graph shows mean +/− SEM of each

group. *, P<0.05 (D) IHC studies confirmed the absence of PPARγ expression in resting and hypertrophic chondrocytes of P0 homozygote PPARγ KO mice compared to control mice. n=4 per group (bar, 100 μm). Figures show one representative experiment of at least four independent experiments.
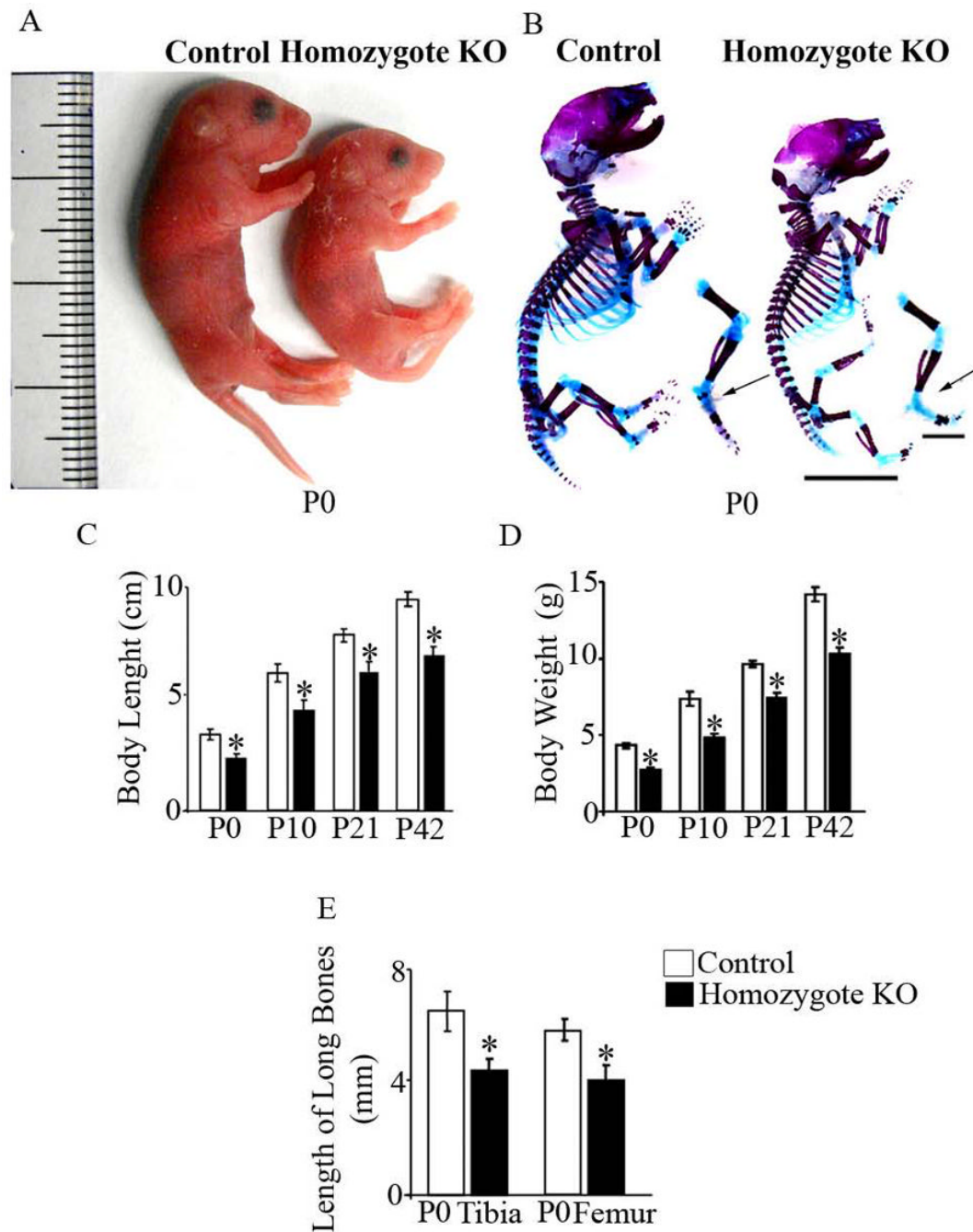
Figure 2.
Cartilage-specific PPARγ KO mice exhibit reduced growth. (A) Newborn homozygote PPARγ KO mice exhibited growth retardation compared to control mice. (B) Skeletal staining demonstrated reduced skeletal size (bar, 10 mm) and length of long bones (bar, 1 mm) in homozygote PPARγ KO mice compared to control mice. Arrows indicate loss of skeletal staining in homozygote PPARγ KO mice. (C) Body length and (D) weight measurements of P0, P10, P21, and P42 mice demonstrated that homozygote PPARγ KO mice exhibit delayed growth compared to control mice. (E) Measurements of P0 mice demonstrated that homozygote PPARγ KO mice have reduced length of tibiae and femurs

compared to control mice. n=6 per group. Figures show one representative experiment of six independent experiments. Bar graph shows mean +/− SEM of each group. *, P<0.05
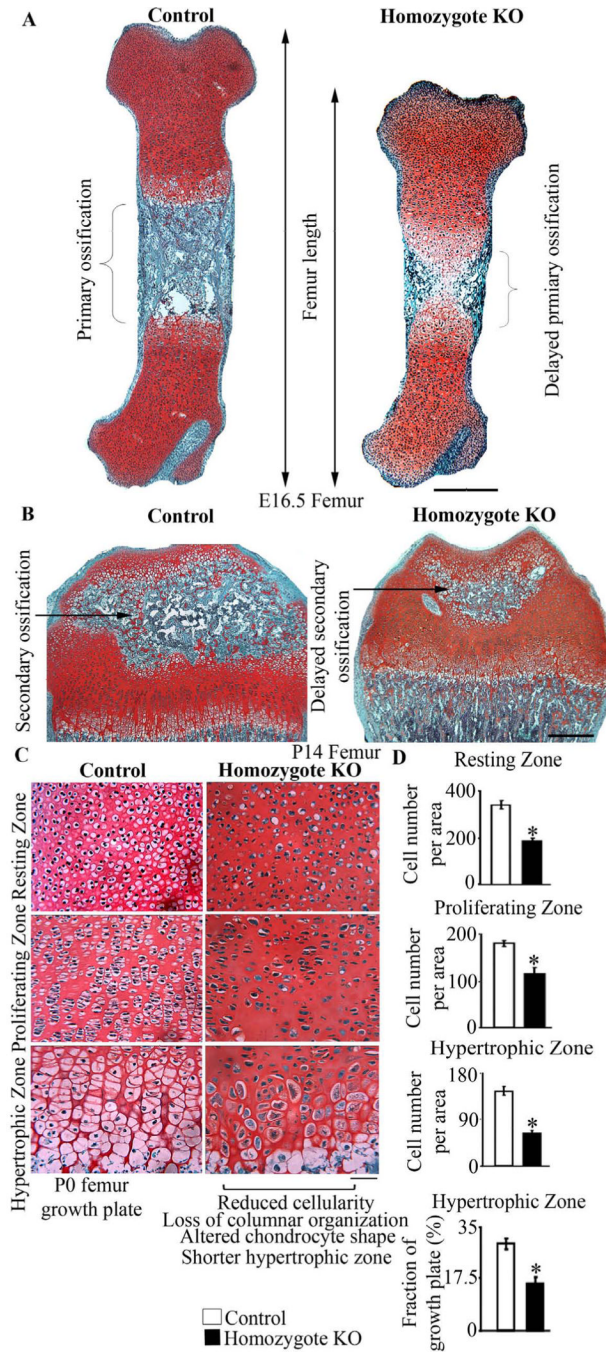
Figure 3.
Cartilage-specific PPARγ KO mice exhibit delayed ossification and disorganization of growth plates. (A) Safranin-O/Fast Green staining demonstrated that E16.5 homozygote PPARγ KO mice exhibit delayed primary ossification compared to control mice. n=6 per group (bar, 500 μm). (B) Safranin-O/Fast Green staining showed delayed secondary ossification in the femurs of P14 homozygote PPARγ KO mice compared to control mice. n=4 per group (bar, 200 μm). (C) Homozygote PPARγ KO growth plates showed disorganization with reduced cellularity in all the three zones loss of columnar organization in the proliferating zone and a shorter hypertrophic zone with altered chondrocyte shape compared to control mice. n=6 per group (bar, 100 μm). (D) Bar graphs show reduced

cellularity in the resting, proliferating, and hypertrophic zones, and shortened hypertrophic zone in homozygote PPARγ KO mice compared to control mice. Figures show one representative experiment of at least four independent experiments. Bar graphs show mean +/− SEM of each group. *, P<0.05
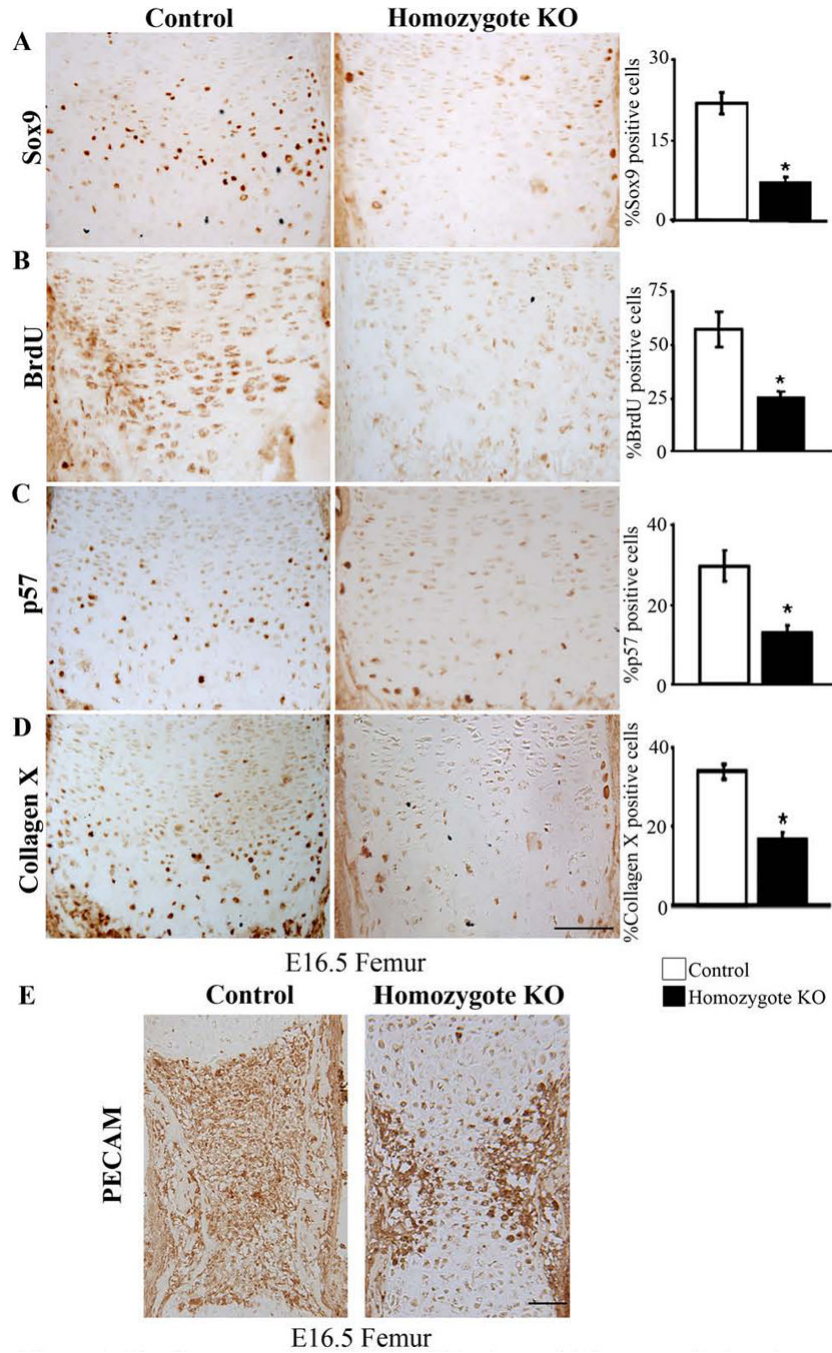
Figure 4.
Cartilage-specific PPARγ KO mice exhibit reduced chondrocyte proliferation, differentiation, hypertrophy and vascular invasion. Staining for (A) Sox9, (B) BrdU, (C) p57, and (D) collagen type X demonstrated reduced chondrocyte proliferation, differentiation and hypertrophy in E16.5 homozygote PPARγ KO mouse femurs compared to control mice. Bar graphs corresponding to IHC analysis show reduced percentage of positive cells for Sox9, BrdU, p57, and collagen type X in homozygote PPARγ KO mice compared to control mice (bar, 200μm). (E) IHC for PECAM confirmed reduced vascularity in the femurs of E16.5 homozygote PPARγ KO mice compared to control mice (bar,

200μm). n=4 per group. Figures show one representative experiment of four independent experiments. Bar graphs show mean +/− SEM of each group. * P<0.05
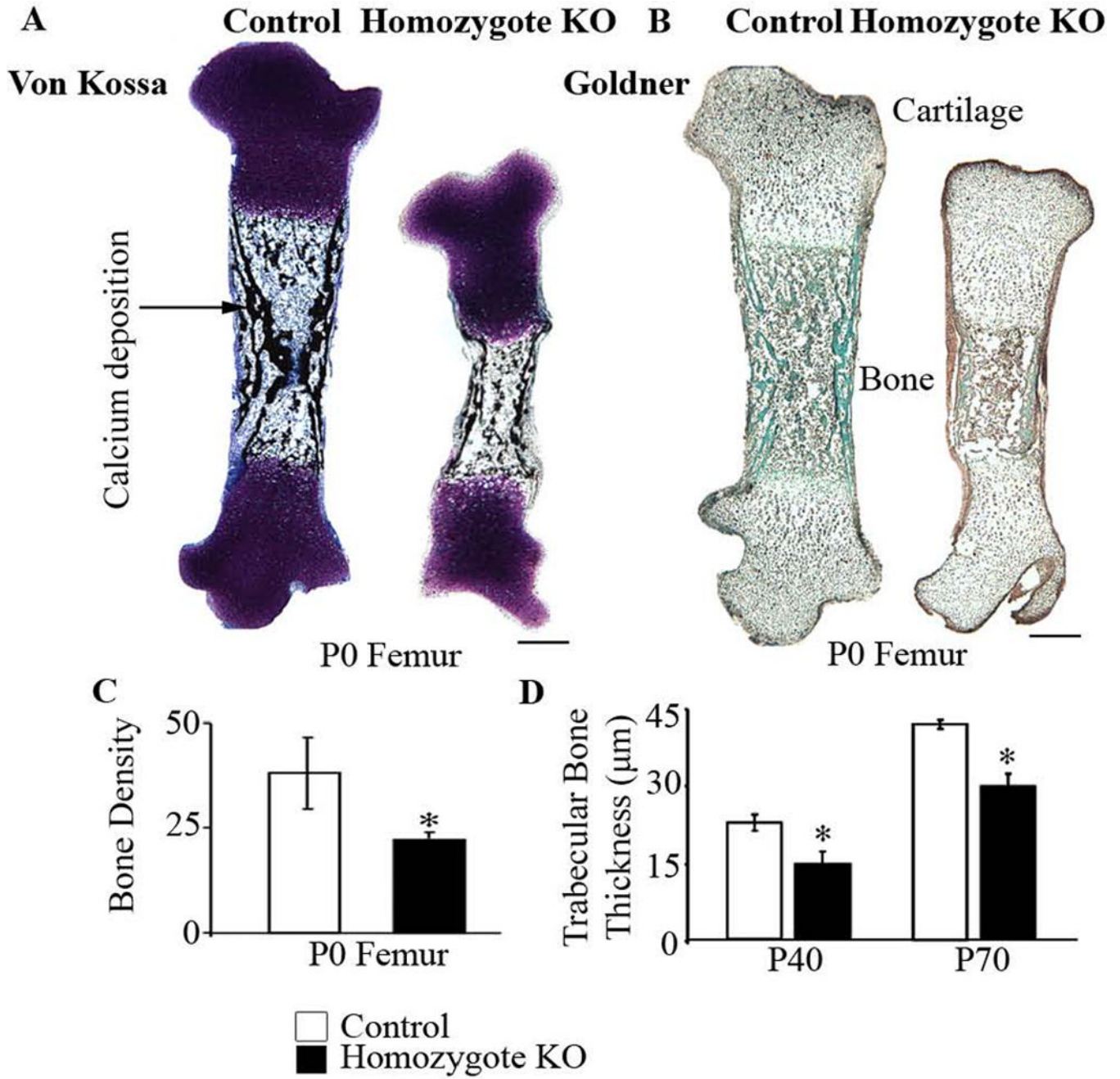
Figure 5.
Cartilage-specific PPARγ KO mice exhibit decreased calcium deposition, bone density and trabecular bone thickness. (A) Von Kossa staining of P0 mouse femurs showed that homozygote PPARγ KO mice exhibit reduced calcium deposition compared to control mice (bar, 500 μm). (B) Goldner staining and (C) bone density quantification using Bioquant Osteo II software demonstrated that the femurs of P0 homozygote PPARγ KO mice show decreased bone density compared to control mice (bar, 500 μm). (D) Quantification of trabecular bone thickness using Bioquant Osteo II software demonstrated that P40 and P70 homozygote PPARγ KO mice exhibit decreased trabecular bone thickness compared to

control mice. n=4 per group. Figures show one representative experiment of four independent experiments. Bar graphs show mean +/− SEM of each group. *, P<0.05
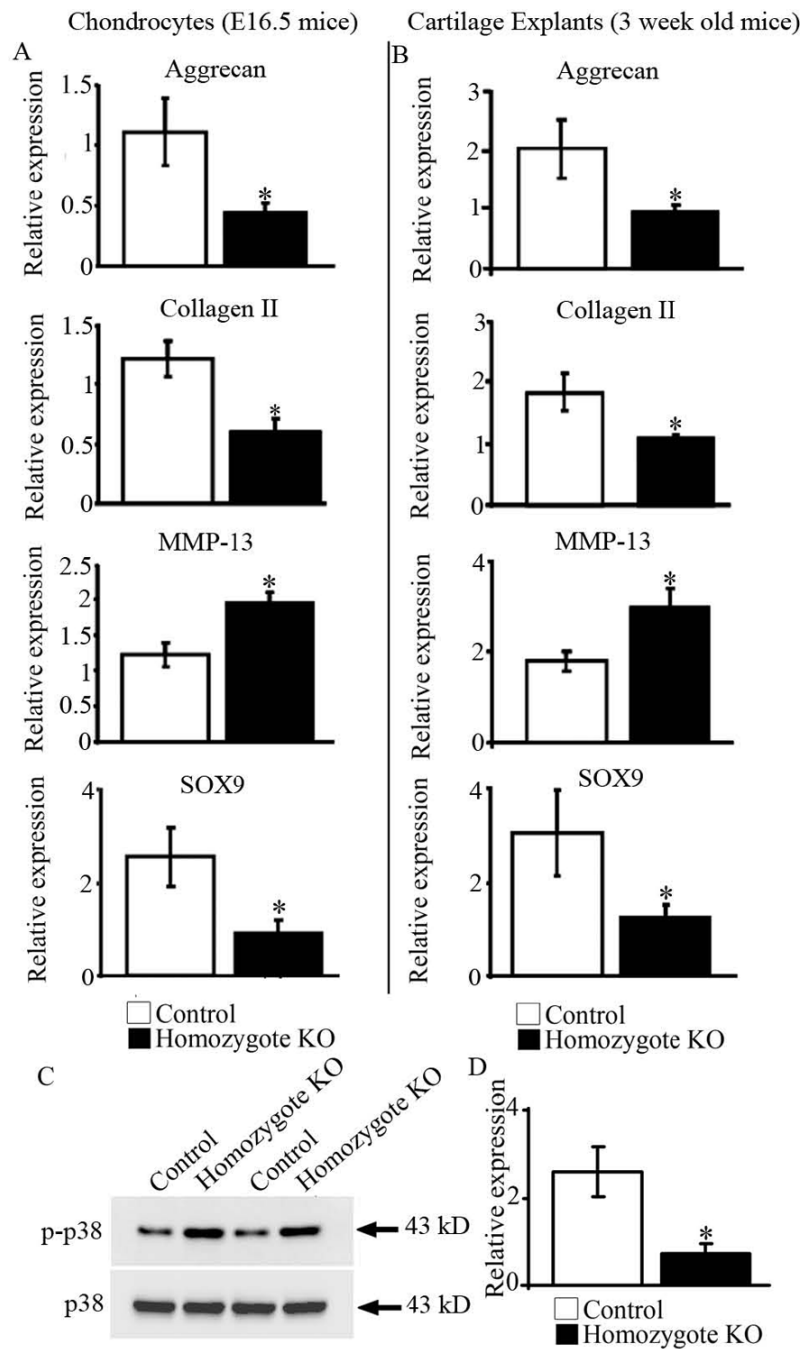
Figure 6.
Genetic ablation of PPARγ results in aberrant expression of endochondral ossification markers, ECM genes and p38 phosphorylation. (A) mRNA expression using RNA isolated from E16.5 mouse chondrocytes indicated decreased expression of aggrecan, collagen type II and SOX9, and increased expression of MMP-13 in homozygote PPARγ KO mice compared to control mice. (B) mRNA expression using RNA isolated from femur head cartilage explants of 3 weeks old mice also indicated decreased expression of aggrecan, collagen type II and SOX9, and increased expression of MMP-13 in homozygote PPARγ KO mice compared to control mice. (C) Increased phosphorylation of p38 was observed in E16.5 mouse chondrocytes isolated from homozygote PPARγ KO mice compared to control

mice. Representative blot from n=4 separate blots is shown. (D) Reduced mRNA expression of Ihh was observed in E16.5 mouse chondrocytes isolated from homozygote PPARγ KO mice compared to control mice. Representative data from n=6 independent isolated chondrocytes and cartilage explants experiments per group. Bar graphs throughout figure show mean +/− SEM of each group. *, P<0.05